Atomic force microscopy of thermal insulation materials with aerogels

Summary of Research

NASA Grant NAG2-1474

April 1, 2001 - June 30, 2002

Principal Investigator
Jonathan Maps

Department of Physics
University of Minnesota Duluth
10 University Dr.
Duluth, MN 55812
Tel. (218) 726-8125, E-mail: jmaps@d.umn.edu

July 27, 2002

Introduction

Superthermal insulation materials developed at NASA Ames Research Center incorporate aerogels into ceramic thermal insulator tiles as a means of improving the thermal resistance of the tiles. These materials hold promise as serving dual functions of thermal protection from atmospheric heating during re-entry, integrated with thermal insulation for cryogen storage.[1] This project has explored the use of atomic force microscopy (AFM) to characterize these materials. AFM has the potential to examine surfaces of insulating materials to nanometer scales. Images have been obtained of a sample of cryoinsulation material prepared at NASA-ARC examined with an atomic force microscope constructed during the course of this project.

Following recent developments, a force microscope was constructed based on a quartz tuning fork (QTF) sensing element.[2] A fine wire attached to the end of one arm of the tuning fork has served as the surface probe. When the tip of the wire is near the surface, the forces between the wire and the surface cause a shift in the resonant frequency away from the free resonance of the tuning fork far from the surface. To image a surface, the tuning fork/probe wire is brought close enough to the surface to shift the resonant frequency up a few hertz from the free resonance, and the the tuning fork is driven at this new resonant frequency. The sample, which is mounted on a piezoelectric tube that provides x-y-z motion, is then rastered beneath the probe. The resonant frequency of the tuning fork varies with x-y position for two main reasons: variations in the probe-surface distance and variations in the surface material properties, chiefly stiffness. The distance is regulated using the z-axis control of the scanner tube to keep the the tuning fork on resonance via a phase-locked feedback loop. The required z-voltage then reflects the general topography of the sample. During the scan the phase and amplitude of the QTF oscillations are also recorded.

If the interaction of the tip with the surface is described by a potential energy function $U_i(z)$, the shift in the resonant frequency for small oscillations can be ascribed to a change in the spring constant of the tuning fork, k. The interaction produces an effective spring constant $k_{\text{eff}} = k + \frac{d^2U_i}{dz^2}\big|_{z_o}$ where z_o is the equilibrium distance of the tip from the surface. For the tuning forks here we have estimated $k \approx 20\,\text{kN/m}$.[3] When the probe is far from the surface (large z_o) the interaction is weakly attractive and diminishing, leading to a small reduction of k_{eff} below k. An increasing repulsive interaction when the tip nears or contacts the surface increases k_{eff}. Since the resonant frequency

of an oscillator can be written as $\sqrt{k_{\text{eff}}/m}$, the frequency should rise when the tip is near or contacting the surface. In practice the oscillation amplitudes are not always small compared to z_o and the interaction should be averaged over the oscillation cycle, but the essential behavior remains.[4]

Tuning fork characteristics

The quartz tuning forks (QTF) used in the force microscope have a nominal resonant frequency of $32768 (= 2^{15})$ Hz. The dimensions of one arm of the tuning fork are $3.6 \times .6 \times .25\,\text{mm}^3$. As supplied in a small vacuum can, we have measured their quality factor to be $Q \approx 90,000$. In air the Q drops to about 10,000, and the resonant frequency drops about 8 Hz. With the addition of the wire probe, affixed with epoxy, the Q drops further to a few thousand and the resonant frequency drops a few thousand Hz due to the additional mass of the epoxy and wire. The QTF was modeled in a standard way as a series R-L-C circuit. The R-L-C model provides a convenient electrical analog of the mechanical properties of the tuning fork. (Its mass m, stiffness or spring constant k, and damping due to internal and external dissipative forces are represented by L, C, and R respectively.) This model is usually further improved by the inclusion of a parallel shunt capacitance C_o corresponding to the package capacitance.[3] See Fig. 1. The admittance was measured as a function of frequency using a signal synthesizer and lock-in amplifier. Typical frequency responses are shown in Fig. 2. Least squares fits to the measurements provided Q and the resonant frequency of the system.

Microscope components and operation

The main mechanical elements of the atomic force microscope were a coarse positioning stage built around a commercial piezoelectric translator and a scanning system, illustrated in Fig. 3. A Burleigh piezoelectric Inchworm motor was used to bring the QTF probe into force-sensing range of the surface from an initial distance of several millimeters. The sample was mounted on a piezoelectric tube scanner. This tube provided x-y scanning of the sample underneath the probe and fine control of z-axis positioning to regulate the resonant frequency via control of the sample/probe separation. Two scanning tubes have been used to image the surface. The tubes have an single inner electrode for axial (z) stretching. The outside surface is divided into four quadrants, which provide x-y scanning motion through bending in response to applied voltages. A 0.25" dia. tube (1" long) was used to scan areas limited to about 0.8μm square. A 0.125" dia tube (1" long) provided larger scanning

areas (potentially 10 μm square) but did not prove to be mechanically robust and failed twice.

The feedback control of the QTF makes use of the characteristic features of the response of a driven damped harmonic oscillator. The oscillation amplitude is proportional to the charge applied to the tuning fork and thus to the current. For convenience we usually consider the admittance of the simple equivalent R-L-C circuit in evaluating the current:

$$Y = \left(R + i(\omega L - \frac{1}{\omega C}) \right)^{-1} = \frac{\omega C}{\sqrt{(\omega RC)^2 + (\omega^2 LC - 1)^2}} e^{-i\delta} \ .$$

With the usual definitions of resonant frequency ${\omega_o}^2 = 1/LC$, and quality factor $Q = \frac{\omega_o}{(R/L)}$, the current due to the tuning fork in response to an applied driving voltage $V_d \cos \omega t$ is

$$I_{\rm tf}(t) = YV_d(t) = \frac{\omega C V_d \cos(\omega t - \delta)}{\sqrt{(\frac{\omega^2}{\omega_o^2} - 1)^2 + (\frac{\omega}{\omega_o Q})^2}} \ .$$

The phase shift δ satisfies $\tan\delta = \frac{\omega^2 LC - 1}{\omega RC} = Q\frac{\omega^2 - \omega_o^2}{\omega\omega_o}$. At resonance the tuning fork acts like a pure resistance, $Y \longrightarrow R^{-1}$, and $\delta = 0$. The current is monitored with a simple op-amp based current-to-voltage converter via a feedback resistor R_f. Off-resonance this voltage can be resolved into two components, one in-phase with the driving voltage (V_i) and another phase-shifted 90° (V_q).

$$\begin{aligned} V_{\rm tf}(t) &= -I_{\rm tf} R_f \\ &= \left[\frac{-\omega C R_f V_d}{\sqrt{(\frac{\omega^2}{\omega_o^2} - 1)^2 + (\frac{\omega}{Q\omega_o})^2}} \right] \cos(\omega t - \delta) \\ &= V_{\rm tf}(\omega) \cos(\omega t - \delta) \\ &= V_{\rm tf}(\omega) \ [\cos\delta \cos(\omega t) \ + \ \sin\delta \sin(\omega t)\,] \\ &= V_i \cos(\omega t) + V_q \sin(\omega t). \end{aligned}$$

The frequency dependent amplitude $V_{\rm tf}(\omega)$ and the phase factors are swept into the coefficients V_i and V_q of the in-phase ($\cos\omega t$) and quadrature ($\sin\omega t$) components. At resonance $V_q = 0$ and V_i measures the amplitude of the resonance. For small deviations from resonance, V_q is proportional to the phase δ since $\sin\delta = \delta - \delta^3/3! + \cdots$.

A lock-in amplifier is used to resolve $V_{\rm tf}(t)$ into these components for use in a phase-locked loop control system.[2,5] The quadrature signal is used as an error signal to indicate departure from the target resonant frequency. The

error signal is integrated via a high voltage op-amp and the result is used to drive the z-axis of the scanner tube to maintain $\delta = 0$, forming the phase-locked loop. The topography is measured by recording the z-axis voltage, $V_z(x, y)$. In practice, the response of the system leaves some small residual error during a scan, so the error (or phase), V_q, and amplitude, V_i are also recorded during a scan. These can detect fine structure in the surface that is obscured by a slow z-response of the control system, noise, slow drift, or by large dynamic z-range of a rough surface.

For small departures from $\delta = 0$, V_q can be interpreted as proportional to the sample slope along the scanning direction. Ridges or sharp valley bottoms in the topography found from $V_z(x, y)$ therefore can appear as abrupt steps or discontinuities in the V_q image. Changes in amplitude can be a consequence of a change in the surface properties (and damping) or limitations on tip motion as a blunt probe attempts to track a sharp surface feature and the tip is no longer the only portion of the probe that may contact the surface.

Operation of the microscope was accomplished largely through software. Coarse positioning, scanning and image acquisition were performed using LabVIEW.

After roughing the QTF probe toward the sample surface by eye with the Inchworm motor, the free resonant frequency was found and the drive oscillator was set to a target frequency typically 5-10 Hz above the free resonance. This would produce comparable in-phase and quadrature (error) signals from the lock-in amplifier. The Inchworm was then stepped repeatedly until the probe was close enough to the surface to shift the QTF resonant frequency to the target frequency, signaled by a drop in V_q. At this point the phase-locked feedback loop could engage to maintain fine z-axis control.

Scanning was performed in a stepwise fashion. Computer-generated voltages were applied to the x and y electrodes of the scanner. After a brief settling time, V_z, V_i, and V_q were recorded and then the x voltage was incremented as appropriate. At the completion of one row, x was ramped back to the origin and the y voltage was incremented. Data was collected only on increasing x ramps to avoid hysteresis problems. During imaging the resonant frequency shifts up from the free resonance were of order 10 Hz. This is expected to correspond to the situation where there is a net repulsive interaction as the probe makes intermittent contact with the sample on each oscillation cycle. For driving voltages used and the observed responses, the amplitude of oscillation is expected to have been in the range of 20 to 100 nm.[3,6] The probes used have been primarily chemically etched tungsten

wires.

Images

A sample of TPS cryoinsulation material, sample 2NNP, supplied by NASA Ames Research Center was used. Images were acquired for scan areas ranging from $(100\text{ nm})^2$ to $(2000\text{ nm})^2$. Representative images, collected from several different macroscopic locations on the sample, are shown in Figs. 4-8. These images show the topography, $z(x, y)$, as determined by V_z in a perspective view and a trio of panes showing z, V_q (the error or phase signal), and V_i (amplitude) viewed from above. The only processing to the data in these images has been the removal of an overall tilt to the z data. The topographic images are generally of poor resolution. While some structure can usually be discerned at all scales, the z images are poorly resolved. This may be a consequence of fluctuating tip conditions or surface modification by the probe during the scan. The phase and amplitude images reveal more successfully finer scale structure.

The correlation between the latter two images and the z topography is clearest in the large area scan, where the z image contains blurry structure that is more sharply outlined in the phase and amplitude images. Since the phase (residual error) signal is roughly proportional to the local slope (dz/dx for these scans) , the phase signal is especially useful in highlighting the meeting of adjacent granular structures where an abrupt change in slope is likely to occur.

Variations in amplitude will also occur at such places. Since the z-feedback lags slightly and does not fully retract the sample from the probe quickly enough, during scans along a steeply rising region the probe can begin to contact the surface more and the amplitude should decrease. On steeply decreasing slopes, the reverse can happen, but typically the amplitude is limited to the free oscillation amplitude. In the case of scans made with cryoinsulation materials, initial amplitudes for a scan were only slightly reduced (10-20%) from the free oscillation amplitude. Variations in sample compressibility can also affect the amplitude as the the effective spring contant varies with location and substantial contact with the sample can increase the damping. A blunt probe will also fail to follow deep narrow topographic features, but be limited by contact of the probe wire at points other than the probe end.

Small range scans with higher spatial sampling rates (images typically consisted of 200^2 to 400^2 pixels) did not result in improved resolution in the scans made on this sample. This is consistent with other efforts to image

aerogel powder glued to a surface.[7] Large scale structures are generally reproducible. The image in Fig. 7, covering 800×800 nm^2 covers an area that includes the area scanned in Fig. 6. Offset voltages were applied to the x and y electrodes to make the centers of these two images correspond to approximately the same location on the sample. The depression and surrounding features visible near the top in the phase and amplitude panes of Fig. 6 can be seen extending further in the larger scan's upper right quadrant.

The TPS cryoinsulation material has proved to be comparatively difficult to image by this technique. As a means of comparison, imaging of highly-oriented pyrolytic graphite is shown in Fig. 9. This material can have stretches of atomically flat surface with steps created when the surface is prepared by peeling layers off with tape. Images of graphite were readily obtained and were reproducible. In addition to the surface steps apparent in the phase and amplitude images, much of the small scale detail reproduces on repeated scans. While imaging graphite, frequency shifts (away from the free resonance) of no more than a 3-4 Hz were achieved before a rapid reduction in amplitude occurred with further attempts to get closer. Presumably the graphite presents a much stiffer surface. In contrast, when imaging the TPS cryoinsulation sample frequency shifts of 10 Hz were achieved with little reduction of oscillation amplitude. As a second comparison, Fig. 10 is an image of an AFM calibration grid used to calibrate the tube scanner's x and y motion. The grid is a replica grating of crossed lines (2160 lines/mm). It, too, readily produced well-defined images upon initial scanning and the phase and amplitude images resolved fine structure. Attempts to image the cryoinsulation sample over areas comparable to the large scan on graphite have yielded unsatisfactory images where significant regions are beyond the range of the z-axis piezo. The combination of limited z-range and surface roughness has been therefore a limiting factor in examining large areas. The roughness also makes it difficult to incorporate high aspect ratio commerically prepared AFM probe tips onto the QTF.

In broad terms the three imaging signals are consistent. In large scans it appears that the signals can show contrasting behavior, where topography does not completely control the content of phase and amplitude images. For example, in Fig. 8 the left side of the image contains substantial topographic (z) variation with remarkably quiet phase and amplitude signals. A sharp boundary appears in the latter two images, where to the right they highlight a granularity that also appears in the topography, but comparatively

weakly. The sharp division of the characteristics suggests a change in sample properties between these two areas.

While scanning force microsopy imaging of these cryoinsulation materials is possible, it has been a comparatively difficult material to image with quartz tuning fork-based probes. Using intermittent contact the simultaneous imaging of topography, and QTF phase and amplitude information provides several potential windows on the surface structure.

Acknowledgments

L. J. Salerno at NASA-Ames suggested the possible use of scanned probe microscopies on these cryoinsulation materials and provided the sample material studied here. J. K. Billa contributed to efforts to characterize the quartz tuning forks as part of a required project toward an M.S. in physics at UMD.

Any opinions, findings, and conclusions or recommendations expressed in this material are those of the author and do not necessarily reflect the views of the National Aeronautics and Space Administration.

References

References

[1] L. J. Salerno, S. M. White, B. P. M. Helvensteijn, "Characterization of an integral themal protection and cryogenic insulation material for advanced space transportation vehicles," 30th International Conference on Environmental Systems, Toulouse, France July 10-13, 2000 (SAE Technical Press Paper Series 2000-01-2236).

[2] Hal Edwards, Larry Taylor, Walter Duncan and Allan J. Melmed, "Fast high resolution atomic force microscopy using a quartz tuning fork as actuator and sensor," J. Appl. Phys. **82**, 980 (1997).

[3] Robert D. Grober, et al. "Fundamental limits to force detection using quartz tuning forks," Rev. Sci. Instrum. **71**, 2776 (2000).

[4] Franz J. Giessibl, "Forces and frequency shifts in atomic-resolution dynamic-force microscopy," Phys. Rev. B **56**, 16010 (1997).

[5] U. Dürig, H. R. Steinauer and N. Blanc, "Dynamic force microscopy by means of the phase-controlled oscillator method," J. Appl. Phys. **82**, 3641 (1997).

[6] Franz J. Giessibl, "High speed force sensor for force microscopyand profilometry utilizing a quartz tuning fork," Rev. Sci. Instrum. **31**, 3956 (1998).

[7] Robert W. Stark et al., "Determination of elastic properties of single aerogel powder particles with the AFM," Ultramicroscopy **75**, 161 (1998).

Figures

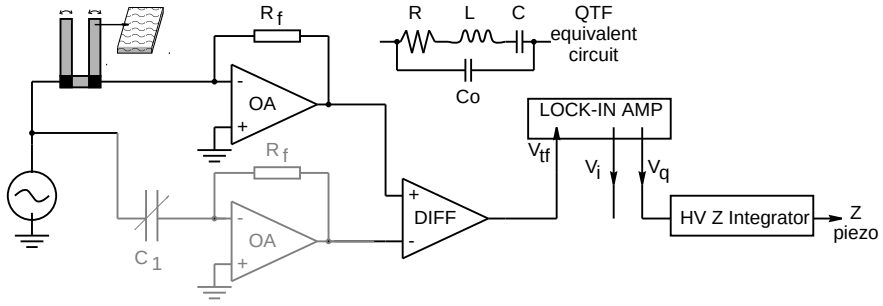

Figure 1: Essential features of tuning fork sensing system and the equivalent circuit. Current through the tuning fork is converted to a voltage by an op-amp (OA). When the wire is attached to the tuning fork, the admittance due to C_o can become a significant fraction compared to the RLC branch of the equivalent circuit. This is nulled out by injecting a matching current through C_1 and using an instrumentation amplifier (DIFF) to subtract the signals. C_1 was adjusted to match C_o by moving far from resonance and nulling V_q. The lock-in reference signal is derived directly from the driving source and is not shown.

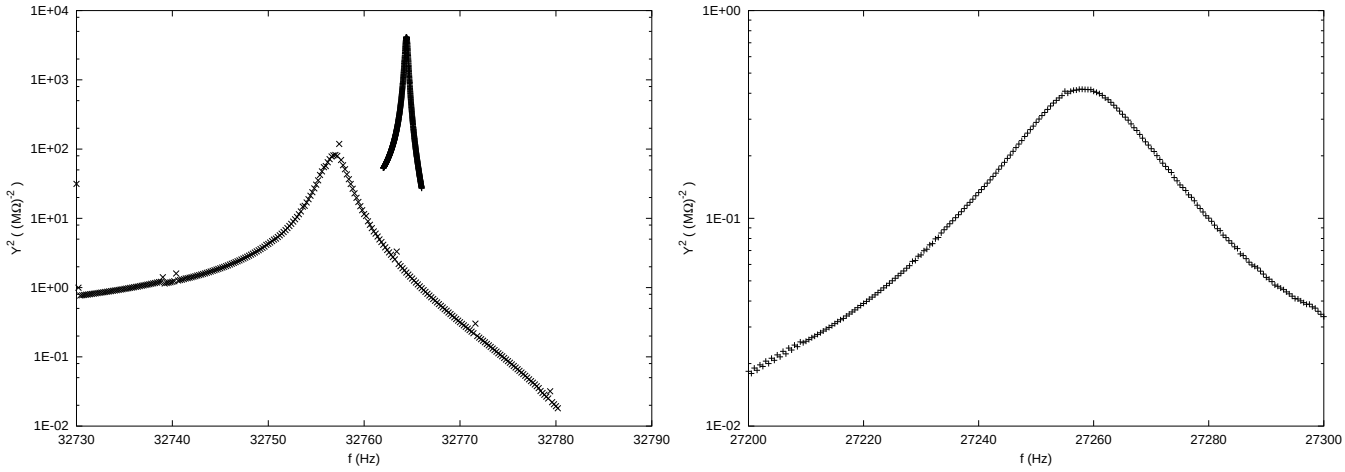

Figure 2: Measured response of tuning tuning forks. Left: square of admittance Y^2 for for tuning fork in vacuum and in air. Right: Y^2 for a tuning fork with wire probe epoxied and mounted for AFM use.

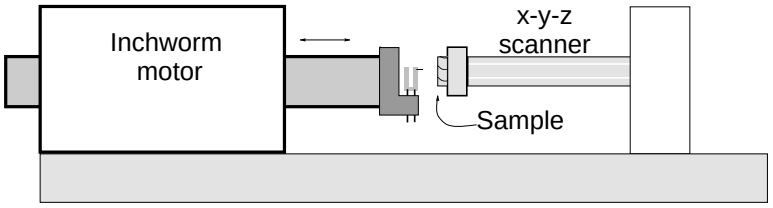

Figure 3: Schematic drawing of the AFM configuration.

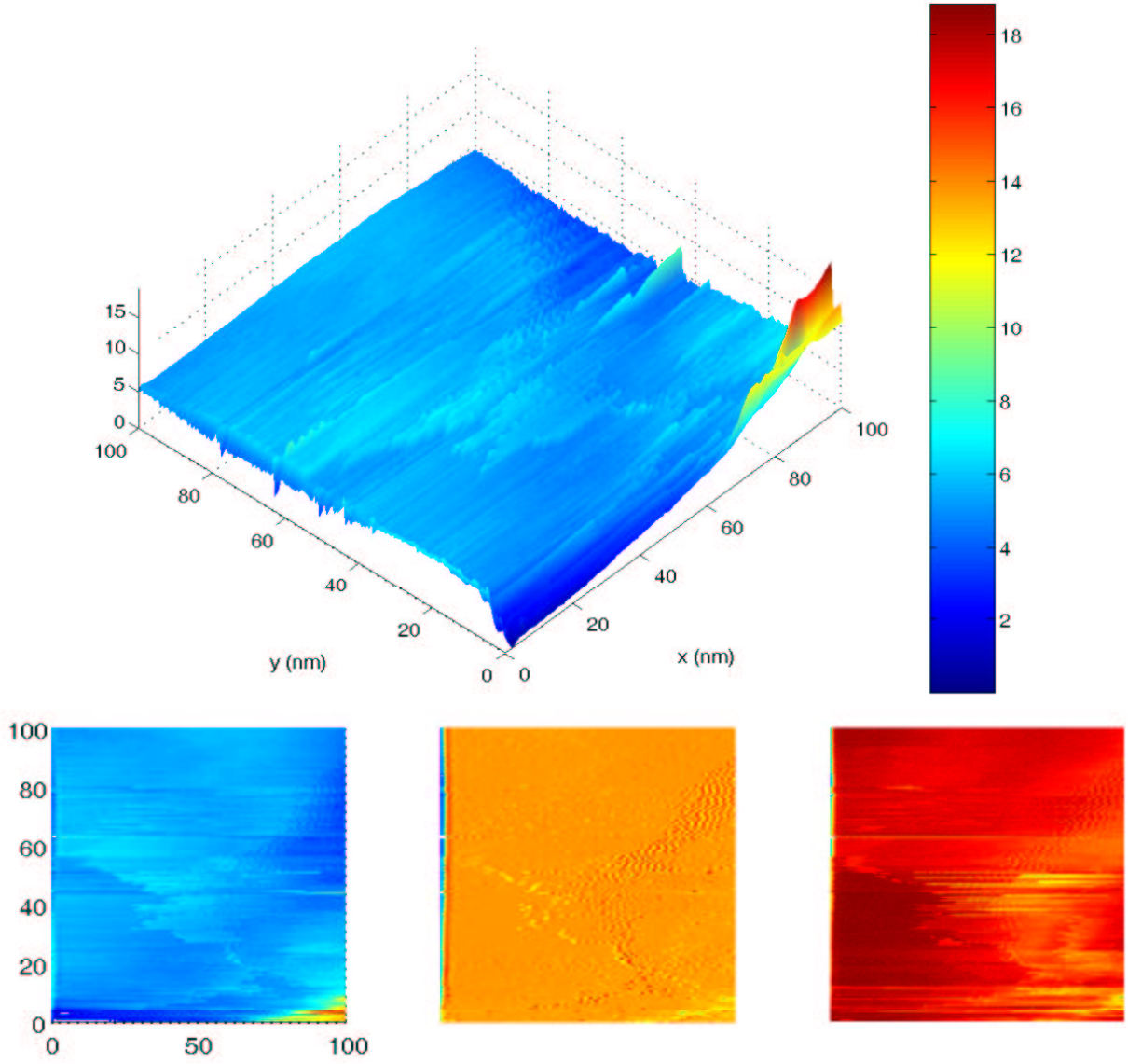

Figure 4: A $(100\,\mathrm{nm})^2$ scan of TPS cryoinsulation sample 2NNP. The top image is $z(x, y)$, while the three lower panes show z, V_q (error or phase signal), and V_i (amplitude).

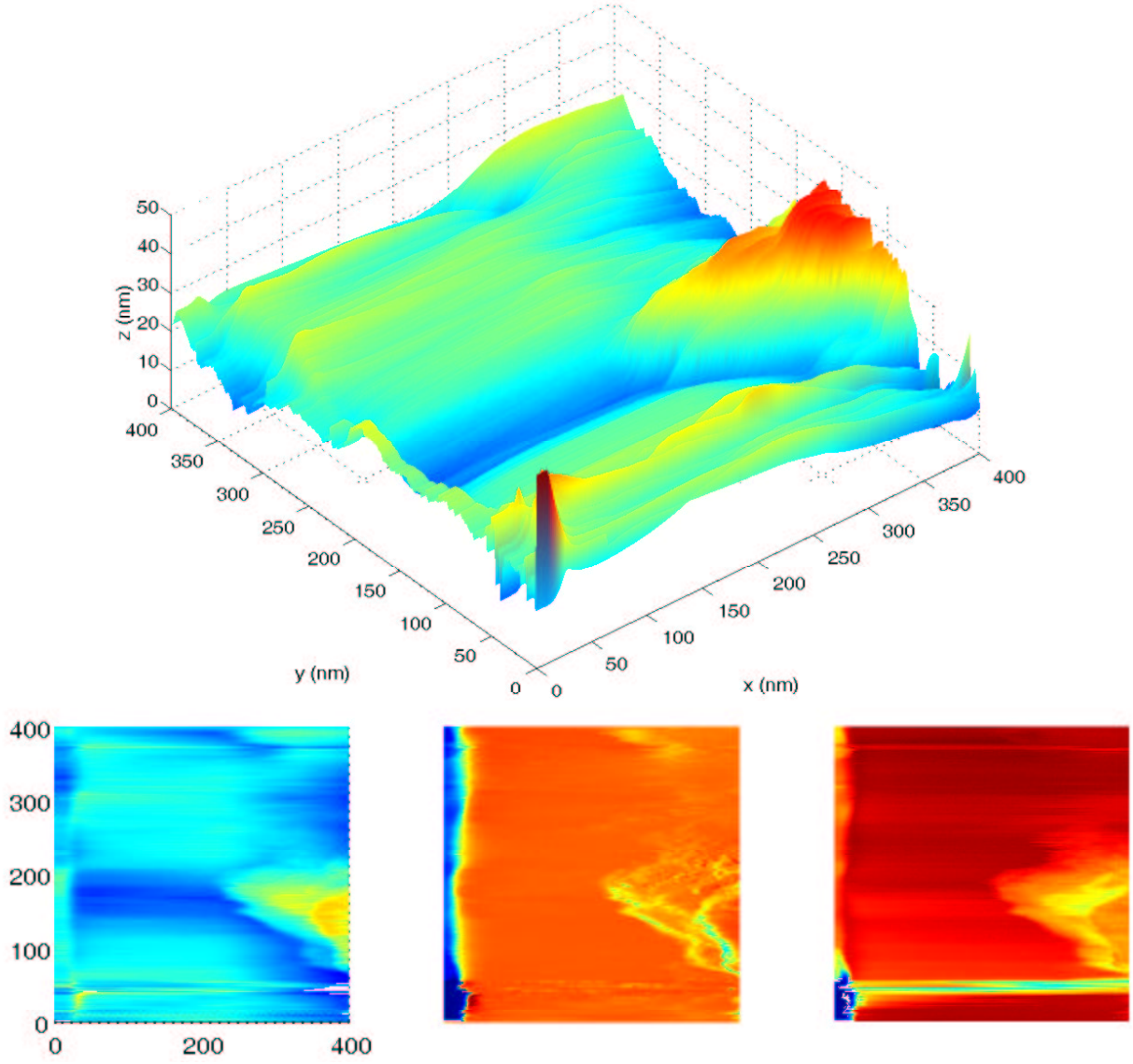

Figure 5: A $(400\,\mathrm{nm})^2$ scan of TPS cryoinsulation sample 2NNP. The three lower panes are again z, V_q (phase), and V_i (amplitude).

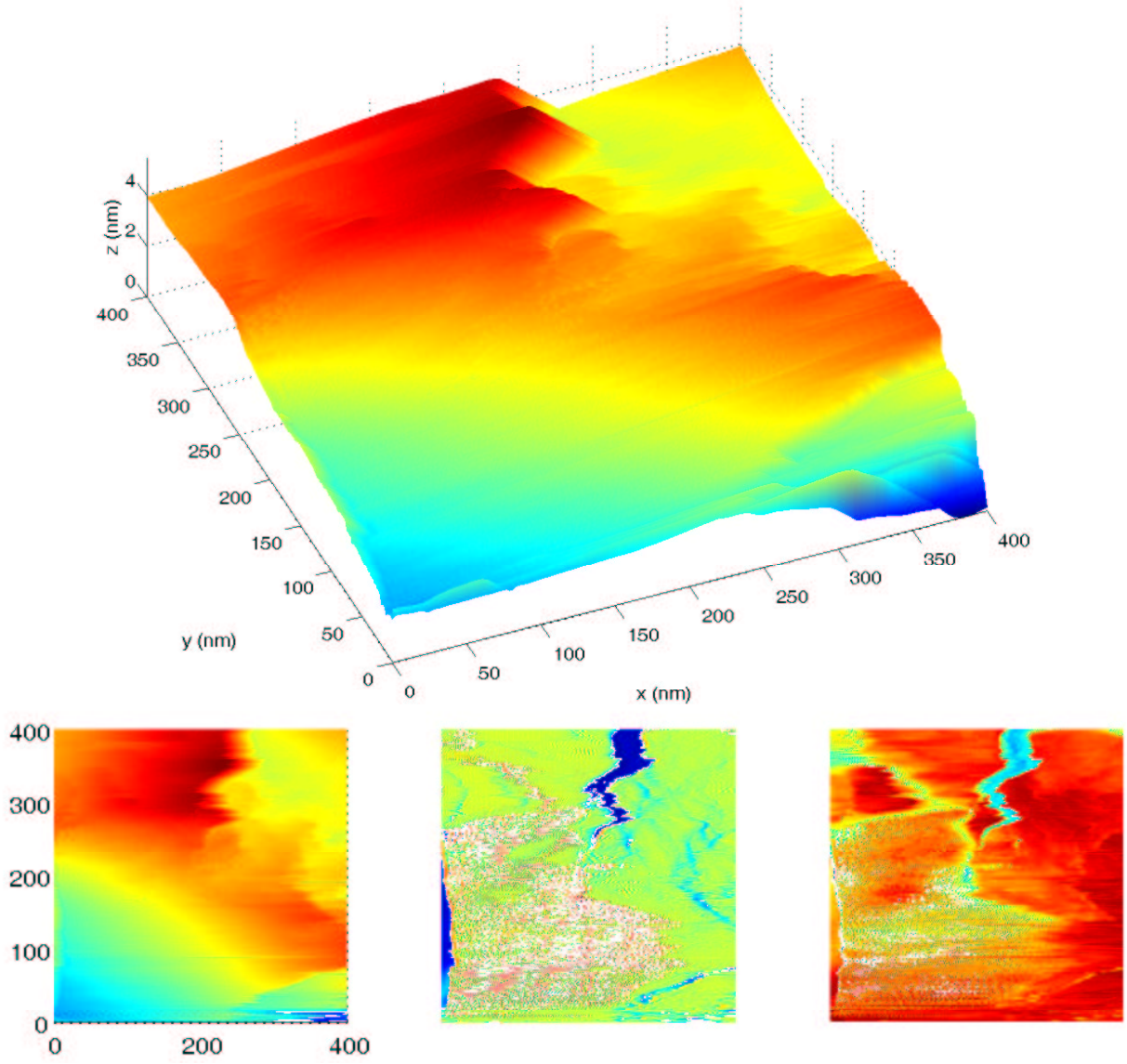

Figure 6: Another $(400\,\mathrm{nm})^2$ scan of TPS cryoinsulation sample 2NNP.

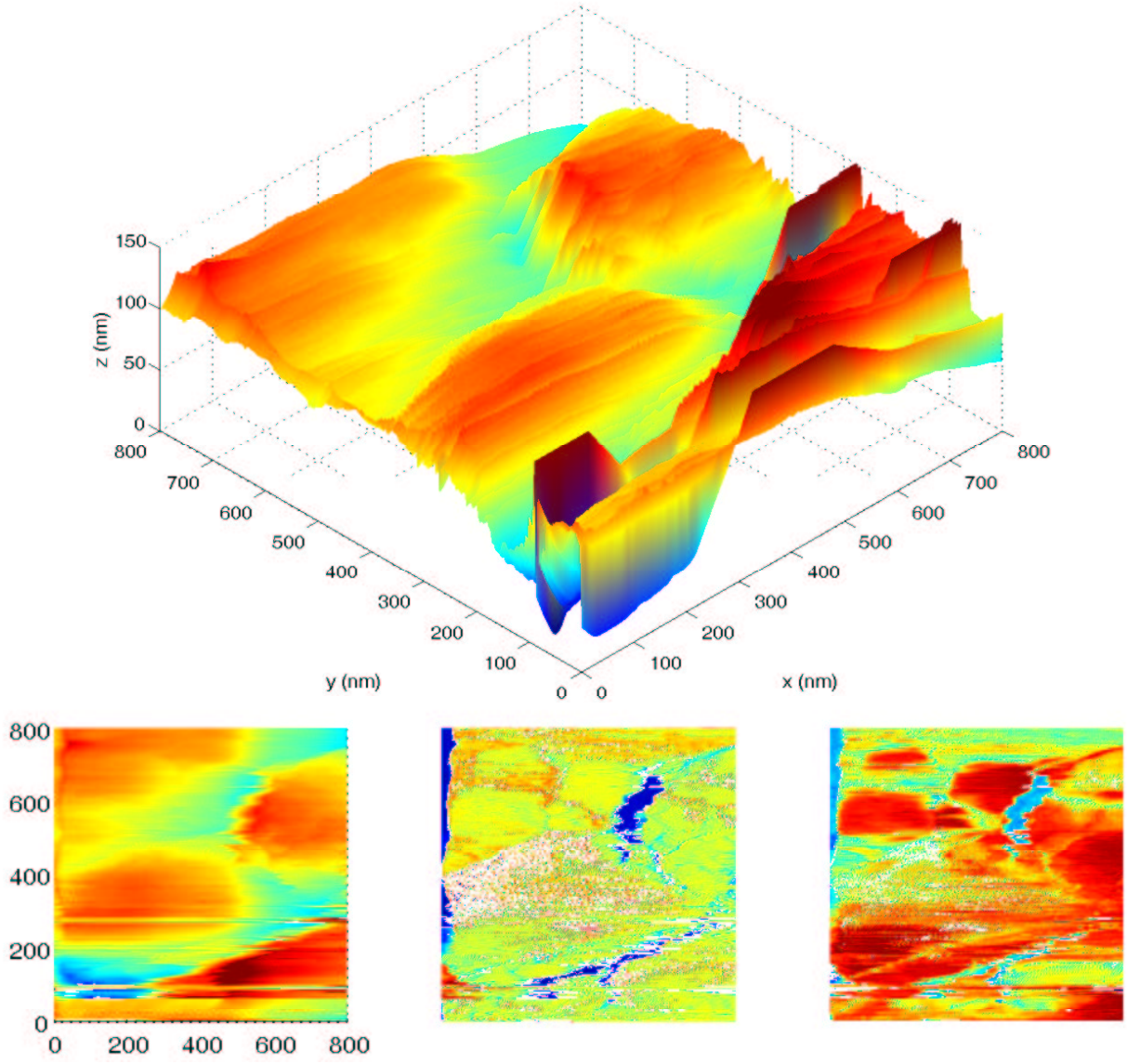

Figure 7: An $(800\,\mathrm{nm})^2$ scan of TPS cryoinsulation sample 2NNP that includes the region scanned in Fig. 6.

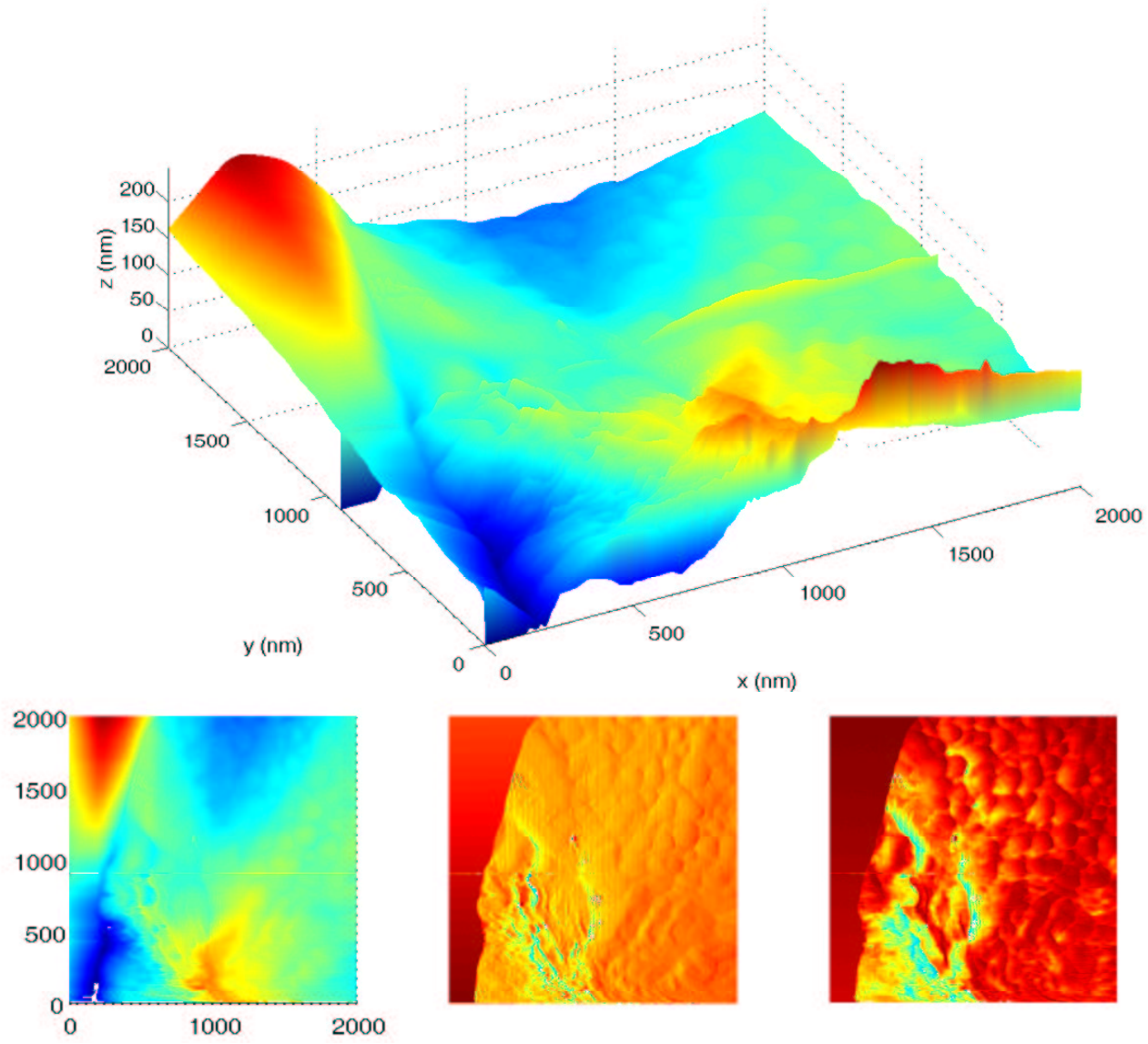

Figure 8: A $(2000\,\mathrm{nm})^2$ scan of TPS cryoinsulation sample 2NNP.

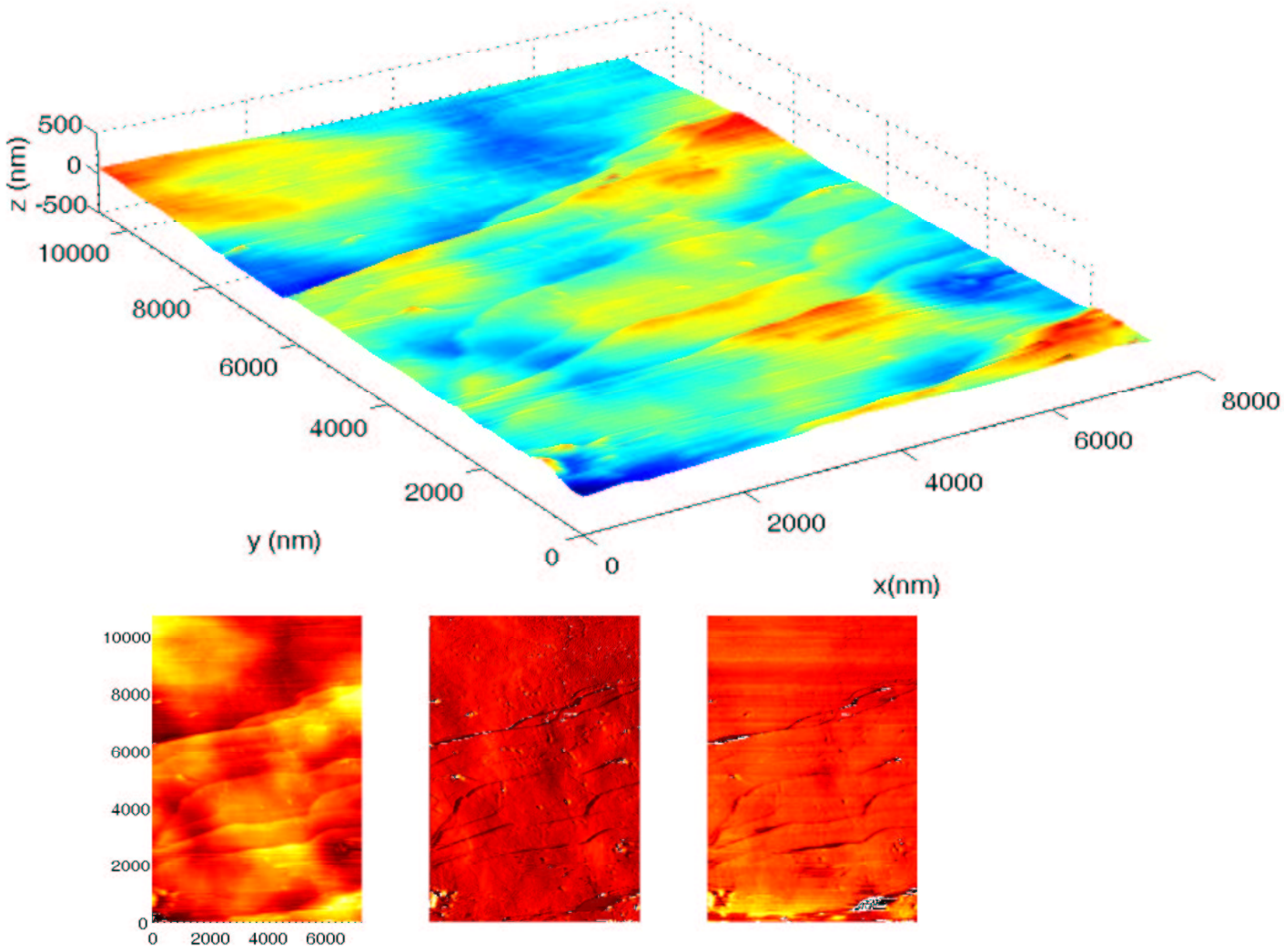

Figure 9: A roughly $7 \times 10\,\mu\mathrm{m}^2$ scan of graphite. The upper image uses a different color mapping than the three lower panes.

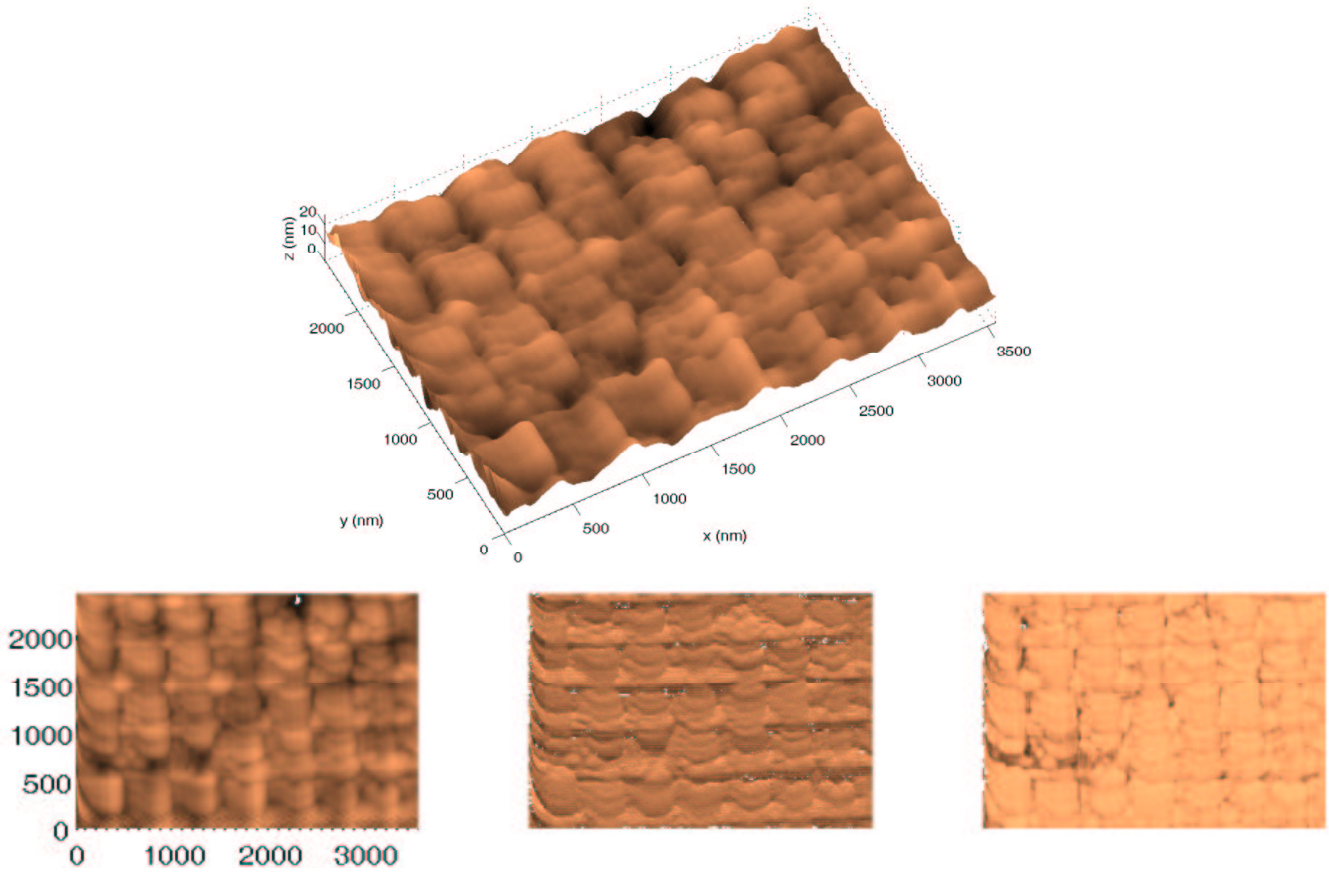

Figure 10: Image of a crossed lines replica grating with nominal line spacing of 460 nm.